JOURNAL OF AIRCRAFT
Vol. 41, No. 2, March–April 2004

Tilt Duct Vertical Takeoff and Landing Uninhabited Aerial Vehicle Concept Design Study

Özlem Armutcuoğlu,* Mehmet Şerif Kavsaoğlu,† and Ozan Tekinalp‡
Middle East Technical University, 06531 Ankara, Turkey

A new autonomously controlled tilt-duct vertical takeoff and landing uninhabited aerial vehicle concept is proposed. This design combines the vertical flight capability of a helicopter and forward flight performance of a fixed-wing conventional aircraft. The two main engines and propellers are located inside the tilting ducts attached to the wing tips. There is a third engine–propeller combination located inside the aft fuselage for pitch and yaw control during hover and transition. The advantages and disadvantages of the ducted propellers are discussed. A conceptual design study is performed including airfoil and geometry selection, initial sizing calculations, estimation of stability and control parameters, etc. Drawings of the aircraft in hover, transition and forward flight modes are presented.

Nomenclature

A = aspect ratio, propeller disk area
b = wing span
C = specific fuel consumption
C_D = drag coefficient
C_{D_α} = variation of drag coefficient with angle of attack
C_{D0} = zero-lift drag coefficient
C_{HT} = horizontal tail volume coefficient
C_L = lift coefficient
C_{L_α} = lift curve slope
C_{l_β} = variation of rolling moment coefficient with angle of sideslip
C_{m_α} = variation of pitching moment coefficient with angle of attack
C_{n_β} = variation of yawing moment coefficient with angle of sideslip
C_{VT} = vertical tail volume coefficient
C_{y_β} = variation of side force coefficient with angle of sideslip
c = chord length
$\bar{c}$ = mean chord length
c_d = airfoil drag coefficient
c_l = airfoil lift coefficient
D = diameter, drag
h = altitude
L = lift, length
P = power
R = range
Re = Reynolds number
S = wing planform area
T = thrust
t = thickness
V = velocity
W = weight
$\bar{X}$ = dimensionless x distance measured from the leading edge of the $\bar{c}$ and normalized with the $\bar{c}$
α = angle of attack
β = sideslip angle
γ = climb angle
η_p = propeller efficiency
Λ = sweep angle
λ = taper ratio
ν = kinematic viscosity
ρ = density

Subscripts

av = available
bhp = brake horsepower
c.g. = center of gravity
e = empty aircraft
f = fuel
HT = horizontal tail
n.p. = neutral point
p = propeller, payload
r = root
TO = takeoff
t = tip
VT = vertical tail
0 = takeoff conditions

Received 26 November 2002; revision received 26 July 2003; accepted for publication 27 July 2003.

*Graduate Student, Department of Aerospace Engineering; currently Ph.D. Student, Graduate School of Industrial Administration, Carnegie–Mellon University, Pittsburgh, PA, 15213.
†Associate Professor, Department of Aerospace Engineering; currently Professor, Department of Aeronautical Engineering, Istanbul Technical University. Senior Member AIAA.
‡Associate Professor, Department of Aerospace Engineering.

Introduction

VERTICAL takeoff and landing (VTOL) capability brings many operational benefits to an aircraft. Whereas conventional transportation depends on airports and long, paved runways, VTOL can be performed in a quite compact area. VTOL aircraft offers a compromise between helicopterlike vertical flight and efficient wing-borne cruise. On the other hand, today uninhabited aerial vehicles (UAVs) have increasing importance and interest in the commercial market. Their applications are being discovered in civilian uses, such as aerial surveys for agriculture, traffic monitoring and pollution control, meteorological data collection, pipeline survey, early forest fire detection, etc. They continue to be very important for the military, especially for reconnaissance purposes. Using UAVs for the dangerous missions can save human lives, and UAVs can be made cheaper than the traditional aircraft.

Since the 1930s, numerous VTOL aircraft configurations have been built and flown with varying degrees of success. This proved that there are many promising approaches to VTOL. These efforts covered many concepts from propeller-driven tail sitters through tilting rotors, tilting wings, deflected slipstream, lift fans, and jet lift types. The main points in these design attempts were to combine

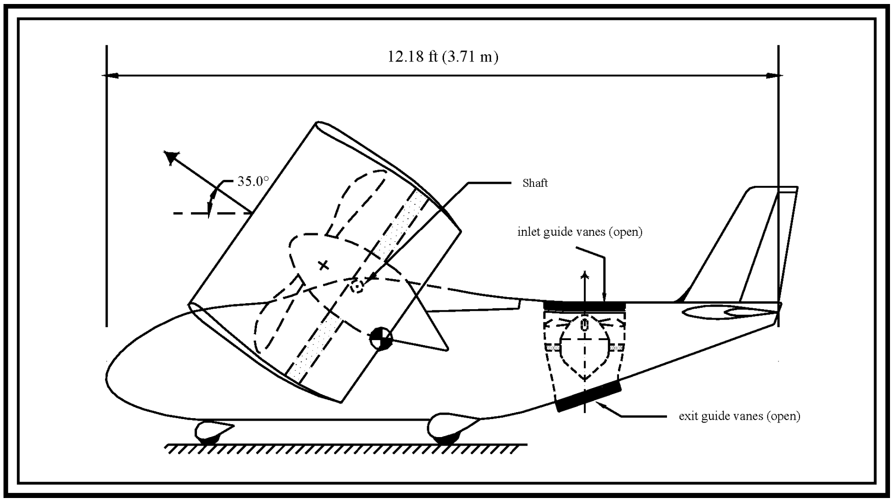

Fig. 1 Side view of tilt-duct VTOL UAV in transition mode, for example, tilt angle = 35 deg.

the vertical flight capability of the helicopter with the superior forward flight performance of the fixed-wing airplane. McCormick[1] gives a brief history of vertical/short takeoff and landing (V/STOL) developments, and specialized books are available on these types of aircraft.[2–4] In the first volume of the *Journal of Aircraft* (1964) various articles appeared related to VTOL aircraft research and development efforts.[5–13] These articles show the importance given to VTOL aircraft in the 1960s. Many VTOL designs utilize tilt-thrust technology. Tilt-thrust vehicles include tilt-jet, tilt-rotor, tilt-wing, tilt-duct, and tilt-propeller aircraft. Seckel discussed the stability and control characteristics of these vehicles.[14] The U.S. Tri-Service V/STOL Programs have made important contributions to the development of tilt-thrust vehicle technologies.[15] Most of these aircraft are crewed. Bell Eagle Eye is an exception, which is a tilt-rotor VTOL UAV.[§]

The benefits of increasing the flow rate by ducting a propeller were first demonstrated in 1931 by the experiments of Stipa in Italy and in 1940 by the analysis of Dickmann[16] in Germany. By adding a duct or shroud to a propeller, one can generate a thrust force on the duct and increase the flow rate through the propeller during axial flight.[8] Decreased loading on the propeller blades can alleviate compressibility effects, cavitation, and noise generation.[8] At angle of attack, the ducted propeller generates much more lift force than an open propeller. Because of mutual interference, the lift force on the ducted propeller can be even larger than on a ring wing and propeller that are separated from each other.[8] Sacks and Burnell[17] reviewed the earlier experimental works. Theories of ducted propellers[18–20] and ring wings[21] were developed. Kriebel and Mendenhall[22] tested the Doak and Bell X22A ducted propellers in the NASA Ames Research Center 40 by 80 ft wind tunnel. They showed that in hovering flight the thrust contribution of the duct was between 50 and 60% of the total thrust. Thompson and Roberts[23] tested the shrouded propellers employed on the XAZ-1 and U.S. Army XV-11A STOL research aircraft. They concluded that significant increases in static and low-speed thrust could be obtained by using the shrouded propellers on these aircraft with little degradation of high-speed performance. They also demonstrated that adaptation of the propeller to the shroud by twisting the propeller to match the inflow velocity profile significantly reduces shroud leading-edge separation and improves performance.

In this work, a tilt-duct VTOL UAV concept is introduced. This design is purposed to add the advantages of VTOL capability to a UAV with autonomous flight capability. Additionally the design should be simple, easy to produce, and fundamentally be constructed using commercial off the shelf parts. The tilt-duct concept has some basic differences from the tilt-rotor concept, such that the propellers are located inside the ducts attached to the wing tips. This provides an endplate effect and separates the rotational wake of propellers from the wing flowfield. Another difference is that the propellers do not need hinges and swash plates, which may lead to cheaper and easier manufacturing.

[§]Data available online at http://www.bellhelicopter.textron.com/ (September 2003).

New Tilt Duct VTOL UAV Concept

In this section, the new tilt-duct VTOL UAV concept is presented. This UAV is shown in Fig. 1. The UAV can takeoff and land as a helicopter and can convert to a propeller-driven airplane when airborne. When the nacelles are in vertical position, it operates as a helicopter. There are two main engines and propellers in ducts located at the tips of the wing. Another ducted engine and propeller mechanism is integrated to the fuselage at the aft. Inlet and exit guide vanes are placed at the both ends of the aft engine's duct. The thrust generated by the aft propeller is vectored using the vanes. Thus, this aft engine is used to control pitch and yaw in hover and transition modes.

In forward flight mode, the main engines tilt angle is 0 deg and the aircraft operates as a conventional propeller-driven airplane. The wings provide necessary lift. Conventional, rudder, aileron, and elevator control surfaces are used. All of the guide vanes, that is, inlet and exit, are closed during forward flight. The aft section engine is used only to obtain electricity in this mode and is disconnected from the aft propeller through an electromagnetic clutch.

Using Ducted Propellers

Advantages of Using Ducts

Ducted propellers are preferred for the design UAV in reference to the following issues:

1) The tilt-duct VTOL UAV does not use rotors, that is, no hinge or swash-plate design. If just uses the regular propellers that can be found in the market. This eases the manufacturing process and reduces the requirement of special expertise. If unducted propellers are used during transitional flight, asymmetric disk loadings may be produced due to the forward speed of the aircraft. Employing cyclic pitch mechanisms can solve this problem. Alternatively, placing the propeller inside a duct may help to eliminate asymmetric disk loadings.

2) Ducts may also help to suppress the vibration effects on the shafts, which are caused by the asymmetric propeller loadings.

3) In tilt-rotor aircraft, during hover, the wing is under the effect of high-pressure, rotational flow coming from the rotor. However, in tilt duct aircraft, the wings will have no interference with the downwash of propellers.

4) The ducts act like endplates and increase the effective aspect ratio of the wing.

Table 1 Methods of obtaining control

Aircraft	Pitch	Roll	Yaw
Conventional airplanes and VTOL in cruise mode	Elevator	Ailerons	Rudder
Helicopter	Longitudinal cyclic	Lateral cyclic	Tail rotor blade pitch
Boeing Vertol VZ-2 tilt wing in hover	Cyclic pitch	Differential collective pitch	Tail rotor collective pitch
XC 142 A tilt wing in hover	Tail propeller thrust	Differential thrust	Aileron deflection
DOAK VZ 4 tilt-duct in hover	Jet exhaust at the tail	Differential thrust	Jet deflection at the tail
X-22A tilt-duct in hover	Differential thrust change between fore and aft propeller sets	Differential thrust change between left and right propeller sets	Deflection of ailerons in ducts
Curtis Wright X-100 tilt propeller in hover	Jet deflection at the tail	Differential pitch between the two propellers	Jet deflection at the tail
Bell X-14 Tilt Jet in hover	Tail jet	Laterally displaced roll jets	Tail jet
Bell–Boeing V-22 Osprey in hover	Longitudinal cyclic pitch	Differential collective pitch	Differential longitudinal cyclic
Present tilt-duct VTOL UAV in hover	Tail propeller thrust	Differential thrust between main engines	Tail engine exhaust vane deflection

5) When ducts are located at the wing tips, the pressure and load distribution will be more balanced from the root to the tips.

6) For small rotors of high disk loading, it is a very attractive idea to enclose the rotor inside a shroud, or duct. The favorable effect is to reduce the induced power for a given thrust. For a small rotor, the shroud may be structurally feasible.[14] Depending on the duct's shape, that is, proportion of the inlet and exit areas, the thrust output may be increased. In hover flight, this may cause an increase in thrust-to-power ratio up to 41% for the same thrust.[4,24]

7) Ducts may act like ring wings to produce lift during the cruising flight, which was observed in X-22A (Ref. 15).

8) It will produce less noise. This may be an advantage, especially in covert reconnaissance flights.

Disadvantages of Using Ducts

The approach of using ducts will also have some disadvantages. These are listed as follows:

1) The ducts will create drag. Although they create an endplate effect and reduce the strength of tip vortex, that is, induced drag, they create drag due to their own wetted area.

2) They will increase the structural weight of the UAV.

3) They will generate large side forces in side winds.

4) The shroud itself becomes a critical element in cruise and, if not properly designed, can seriously affect propulsive efficiency. Tests by Hamilton Standard show that a shrouded propeller can produce the same propulsive efficiency as an open propeller up to Mach = 0.5 provided a thin lip is used. Unfortunately, a well-rounded lip is required in hover and a good, fixed-geometry compromise is difficult to achieve.[15]

5) If horizontally opposed piston engines are used, it may be somewhat difficult to handle them at low velocities. The horizontally opposed engines vibrate at low speeds. In the case of the tilt-duct VTOL UAV, the engines are located at the centerline of the ducts by means of five airfoil profiled sticks–clip combination. Thus, the reaction of the duct–engine combination should be tested for vibration durability at low speeds.

Control Policy

During the hover and transition modes, pitch and yaw is controlled using the vectored thrust provided by the aft engine. Thrust vector of the aft engine can be adjusted by means of exit guide vanes, propeller pitch, and engine throttle. In the present design, aft engines thrust vector is upward and can be tilted left or right for yaw control. Therefore, the c.g. location needs to be aft of the main engines lift vector. Alternatively, downward thrust from the aft engine can be considered, which allows placement of the c.g. forward of the main engines lift vector. In hover and transition modes, roll control is achieved by differential thrust realized at the main engines. This is achieved by differential propeller pitch control between the right and left engines. Fixed-pitch propellers can be used to reduce cost. For this case, roll control can be obtained by differential throttle control between the left and right engines. However, throttle control is known to be a slowly responding phenomenon and should be avoided.

As the ducts are tilted forward, the aircraft accelerates. The wings generate lift as speed increases. This is the transition mode. At the beginning of transition, the hover mode is dominant. As the aircraft gains speed, control is gradually switched to aerodynamic control surfaces.

When the nacelles become horizontal, the aircraft operates as a conventional propeller-driven airplane. The wings provide necessary lift. Conventional, rudder, aileron, and elevator control surfaces are used.

In Table 1 the control methods of the present design are compared with the control methods used in different VTOL aircraft types. In conventional airplanes, control moments are produced by using relatively small forces and long moment arms. On the other hand, in classical helicopters pitch and roll control moments are produced by using short moment arms and larger forces. The first approach seems to be better and may be preferred for producing control moments of the VTOL aircraft during hover and transition.

Design Study

During the design study, the theories and methods described in Refs.[25–27] are utilized. Some of the calculations are performed by using the AAA program.[28] A summary of the results will be presented. The details of the calculations are available in Ref. 29.

Requirements

The aircraft is to carry a television camera as payload, so the payload weight is kept small, approximately at about 10 kg (22.05 lb). The cruise height is set to be 2000 m (6562 ft). The maximum stall speed at 1000-m (3281 ft) altitude is selected as 92.60 km/hr (50 kn). The cruising speed should be greater than 157.42 km/hr (85 kn), and the range should be greater than 1000 km (540 nm).

Mission Profile

The mission profile of the tilt-duct VTOL UAV is given in Fig. 2. The flight segments are as follows: 0–1, vertical takeoff; 1–2, transition; 2–3, climb; 3–4, cruise; 4–5, descend; 5–6, transition, and 6–7, vertical landing (Fig. 2).

Airfoil and Geometry Selection

After the first guess calculations, the cruise speed is estimated as 37.80 m/s (124 ft/s) and mean chord length as 0.54 m (1.77 ft). When the standard atmosphere kinematic viscosity at the cruising altitude (2000 m) is used, the design Reynolds number is calculated as

$$Re = \frac{V_{cr} c}{\nu} = \frac{(124)(1.77)}{0.1846 \times 10^{-3}} \cong 1.2 \times 10^6$$

In Table 2, the selected geometric parameters of the wing, the horizontal tail, and the vertical tail are shown. The Eppler E-583 airfoil[30] is selected as the wing airfoil. This airfoil is suitable for our design Reynolds number, has high pressure recovery on both sides, and does not show bubble formation at our design conditions.[30] It is a 16.5% thick airfoil, thus, provides room for the necessary subsystems inside the wing. The Eppler E-521 airfoil[30] is selected for the vertical and horizontal tails. This is a 13.78% symmetric airfoil suitable for tail surfaces. The geometries of E-583 and E-521 airfoils are shown in Figs. 3 and 4, and their basic features are listed in Table 3.

To reach a compromise between aerodynamic efficiency and structural weight, the wing aspect ratio is selected as 6.0. The ducts at the wing tips act as endplates, and this improves the aerodynamic efficiency by making effective aspect ratio up to about 20% higher than the geometric aspect ratio.[25] For the wing vertical location, a high wing configuration is selected to provide sufficient ground clearance for the ducted propellers.

Horsepower to Weight Ratio and Wing Loading

If the horse power to weight ratio is high, then the aircraft will accelerate more quickly, climb more rapidly, reach a higher maximum velocity, and achieve higher turn rates. However, a higher horse power to weight ratio means a larger engine, which consumes more fuel. Hence, the cost will increase. The literature survey yields horse power to weight ratio of Bell V-22 Osprey as 0.252 hp/lb (42.25 W/N) and horse power to weight ratio of Bell/Augusta 609 as 0.231 hp/lb (38.73 W/N). For the present design the horse power to weight ratio is selected as horse power to weight = 0.212 hp/lb (35.54 W/N). A typical wing loading value is around 11 lb/ft^2 (526.68 N/m^2) for small home-built airplanes.[25] To satisfy the stall speed requirement of 50 kn (92.60 km/hr) at 1000-m (3280-ft) altitude, the wing loading is selected as

$$W/S_{\text{TO}} = 12\ \text{lb/ft}^2 (574.56\ \text{N/m}^2)$$

Propulsion

Two, two-blade propellers with individual engines are used. They are directly connected, housed in nacelles, and attached to the tips of the wings with a tilt mechanism. Tilt mechanism is achieved via a center shaft, driven with a single actuator. A four-blade aft propeller, with inlet and exit guide vanes, is installed inside the fuselage. Guide vanes are closed during the cruise. During hover and transition, exit guide vanes are used for thrust vectoring (Fig. 1).

Table 2 Geometry parameters for wing, horizontal tail, and vertical tail

Parameter	Wing	Horizontal tail	Vertical tail
Airfoil	E-583	E-521	E-521
Airfoil t/c	%16.5	%13.78	%13.78
A	6	4	1.6
λ	1	0.5	0.5
Sweep $\Lambda_{l.e.}$, deg	0	17	30
Dihedral	None	None	None
Twist	None	None	None
Incidence, deg	3	0	0
Type	High wing	Conventional	Conventional
Tips	Cutoff	Hoerner	Sharp

Table 3 Basic features of the selected airfoils

	Air foil	
	E-583	E-521
Maximum t/c at	0.38 c	0.30 c
$c_{d,\min}$	0.0053 at $\alpha \cong -3$ deg	0.0058 at $\alpha = 0$ deg
$c_l)_{c_{d,\min}}$	0.28	0.0
$c_{\ell,\max}$	1.45 at $\alpha \cong 11$ deg	1.0 at $\alpha \cong 10$ deg
$c_l/c_d)_{\max}$	$1.19/0.0095 \cong 125$ at $\alpha \cong 6.5$ deg	$0.55/0.0088 \cong 62.5$ at $\alpha \cong 5.2$ deg
$c_{\ell,\text{design}}$	1.0 at $\alpha \cong 4.0$ deg	0.0 at $\alpha = 0$ deg
$\alpha)_{c_l=0}$	−5.2 deg	0.0 deg

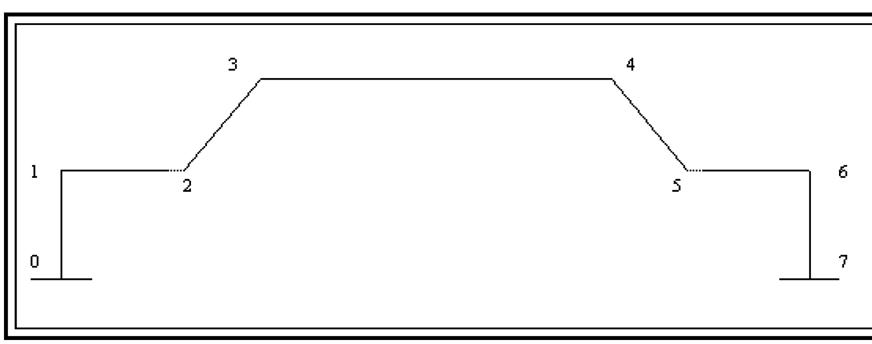

Fig. 2 Mission profile of tilt-duct VTOL UAV.

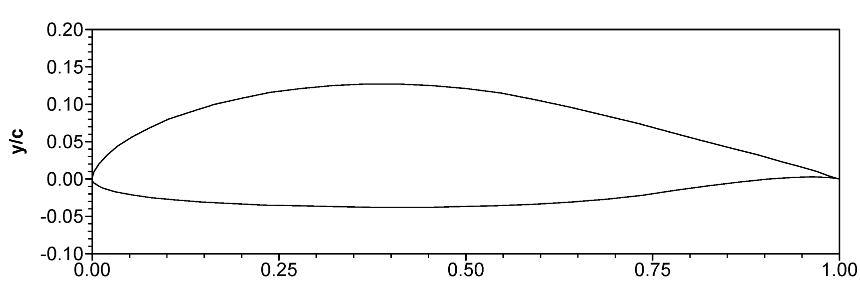

Fig. 3 E-583 airfoil.

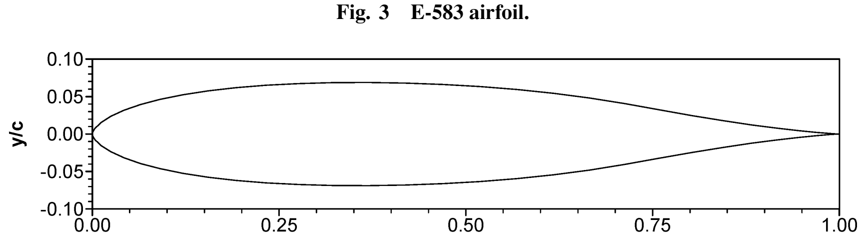

Fig. 4 E-521 airfoil.

For the two main engines, the Limbach L-275E is considered. This is a two-cylinder, horizontally opposed, two-stroke, air-cooled piston engine.[31] It weighs 16.54 lb (73.6 N) and produces 24 hp (18 kW) at 7300 rpm. For the aft engine, the Limbach L-90E is found to be appropriate. This is also a two-cylinder, horizontally opposed, two-stroke, air-cooled piston engine, which weighs 8.82 lb (39.2 N) and produces 4.0 hp (2.9 kW) at 7000 rpm.

It is found appropriate to place a gearbox between each main engine and its propeller such that propellers rotate three times slower than the engine shaft. Thus, when the engines rotate at 7300 rpm, propellers rotate at 2433 rpm. The propeller diameter is selected as $D_p = 3.94$ ft = 1.2 m. It is checked that sonic speed should not occur at the propeller tips and this propeller diameter is suitable with the engine power according to the methods described in Refs. 1 and 25.

To estimate the maximum static thrust, first the idealized momentum theory is used.[1] This theory gives the following expression for the maximum static thrust of an open propeller:

$$T = P_{i0}^{\frac{2}{3}}(2\rho A)^{\frac{1}{3}}$$

where P_{i0} is the static induced power and A is the propeller disk area. When $P_{i0} = 24$ hp = 17,900 W is used, the sea-level, open-propeller thrust of each engine can be found as 961 N (216 lb). This value is the theoretical upper limit and does not account for the losses. A more accurate calculation can be made using the Hamilton Standard propeller charts given in Ref. 32. When an activity factor = 120 and propeller design lift coefficient of $C_L = 0.5$ are assumed and $P = 24$ hp = 17,900 W at 2433 rpm is used, the sea-level, open-propeller static thrust of each engine is found as 699 N (157 lb). A correction to this value needs to be made for obtaining the static thrust of a ducted propeller. For the power to thrust ratio, a simple analysis based on the momentum theory gives[24]

$$P/T = \tfrac{1}{4}\left[3V + \sqrt{V^2 + 4\phi(T/\rho A)}\right]$$

where V is the axial air velocity into the duct and ϕ is the ratio of the propeller disk area to the exhaust area,

$$\phi = A/A_{\text{exhaust}}$$

For an open propeller, ϕ is equal to 2, and for a constant area duct, ϕ is equal to 1. At the static condition, $V = 0$,

$$T = (4P^2\rho A/\phi)^{\frac{1}{3}}$$

For the present ducted propellers, ϕ is equal to 1. For the same power, the static thrust of a ducted propeller can be obtained from the static thrust of the corresponding open propeller by using the following equation:

$$T_{\text{ducted}\,(\phi=1)} = 2^{\frac{1}{3}}T_{\text{open}(\phi=2)} = 1.26T_{\text{open}(\phi=2)}$$

From here, the sea-level static thrust of each engine can be calculated as $1.26 \times 699 = 881$ N. Thus, the total static thrust is estimated as $881 \times 2 = 1762$ N = 396 lb.

Sizing

From the selected horsepower (HP) to weight ratio, the maximum take of weight can be calculated as

$$W_0 = \text{HP}_0 \Big/ \left.\frac{\text{HP}}{W}\right)_0 = \frac{24\,\text{HP}^*2}{0.212} = 226.2\,\text{lb} = 1006.1\,\text{N}$$

Then, the sea level thrust to weight ratio during hover becomes

$$\left.\frac{T}{W}\right)_0 = \frac{1762}{1006.1} = 1.75$$

Empty weight is calculated from the following expression.[29]

$$W_e/W_o = 1.15(W_o)^{-0.1}$$

where W_0 is in pounds. This gives

$$W_e/W_o = 151.5\text{ lb (673.9 N)}$$

Then the fuel weight can be calculated from the sizing equation[25] for a given payload weight:

$$W_o = \frac{W_{\text{payload}}}{1 - (W_f/W_o) - (W_e/W_o)}$$

Range is calculated by using the cruise segment weight fraction, W_4/W_3, which can be obtained from the following relationships[25]

$$W_f/W_0 = 1.06[1 - (W_7/W_0)]$$

and

$$W_7/W_0 = (W_7/W_5)(W_5/W_4)(W_4/W_3)(W_3/W_2)(W_2/W_0)$$

Then Breguet's range equation is used to calculate the range:

$$\frac{W_4}{W_3} = \exp\left[\frac{-RC_{\text{bhp}}}{550\eta_p(L/D)3600}\right]$$

Here, the specific fuel consumption C_{bhp} is in pounds force (fuel) per horse power per hour and the range R is in feet.

During the range calculations the following assumptions are made:
$V_{\text{cruise}} = 150$ ft/s (46 m/s), $L/D)_{\text{cruise}} = 7.25$, $C_{\text{bhp}} = 0.5$ lbf (fuel)/hp · h [0.003 N(fuel)/W · h], $\eta_p = 0.8$, $h_{\text{cruise}} = 2000$ m (6562 ft), $W_7/W_5 = 0.96$, $W_5/W_4 = 0.99$, $W_3/W_2 = 0.99$, and $W_2/W_0 = 0.99$. For different payload/fuel combinations the results of the sizing calculations is shown in Table 4. A geometry sizing study is also performed, and the main results are summarized in Table 5.

Landing Gear

A nonretractable, tricycle-type landing gear arrangement is designed. Each unit is equipped with oleo pneumatic shock absorbers. Disk brakes are installed on the main wheels. Aerodynamic cabs are used to reduce drag. The main wheel's diameter is 10 in. (25.4 cm), and the nose wheel diameter is 8 in. (20.32 cm).

Table 4 Sizing study results

W_0, lbf	W_p, lbf	W_e, lbf	W_f, lbf	$W_f + W_p$, lbf	Range, n mile (km)
226.6	22.05	151.5	53.05	75.1	598 (1106)
226.6	30	151.5	45.1	75.1	440 (816)
226.6	40	151.5	35.1	75.1	251 (466)

Table 5 Geometric dimensions of the wing, fuselage, and tails

Component	Quantity
Wing	
S_w	18.88 ft^2 (1.754 m^2)
b_w	10.64 ft (3.24 m)
c_w	1.77 ft (0.541 m)
Fuselage	
L_{fus}	12.18 ft (3.71 m)
D_{fus}	2.13 ft (0.65 m)
Horizontal tail	
L_{HT}	6.33 ft (1.93 m)
C_{HT}	1.29
S_{HT}	6.8 ft^2 (0.63 m^2)
b_{HT}	5.21 ft (1.59 m)
c_r	1.74 ft (0.53 m)
c_t	0.87 ft (0.26 m)
Vertical tail	
L_{VT}	6.58 ft (2.00 m)
C_{VT}	0.09
S_{VT}	2.75 ft^2(0.25 m^2)
b_{VT}	2.1 ft (0.53 m)
c_r	1.75 ft (0.53 m)
c_t	0.87 ft (0.27 m)

Table 6 Component wetted surface areas and volumes[a]

Parameter	Wing	Horizontal tail	Vertical tail	Fuselage	Nacelles	Total
S_{wet}	39.94 ft^2 (3.62 m^2)	13.92 ft^2 (1.29 m^2)	5.63 ft^2 (0.52 m^2)	68.78 ft^2 (6.39 m^2)	174.5 ft^2 (16.21 m^2)	302.77 ft^2 (28.13 m^2)
S_{wet}/S_{ref}	2.12	0.74	0.30	3.64	9.24	16.04
Volume	2.59 ft^3 (0.07 m^3)	0.701 ft^3 (0.021 m^3)	0.287 ft^3 (0.008 m^3)	28.50 ft^3 (0.81 m^3)	92.03 ft^3 (2.61 m^3)	122.11 ft^3 (3.52 m^3)

[a] $S_{ref} = S_w = 18.88$ ft (1.74 m^2).

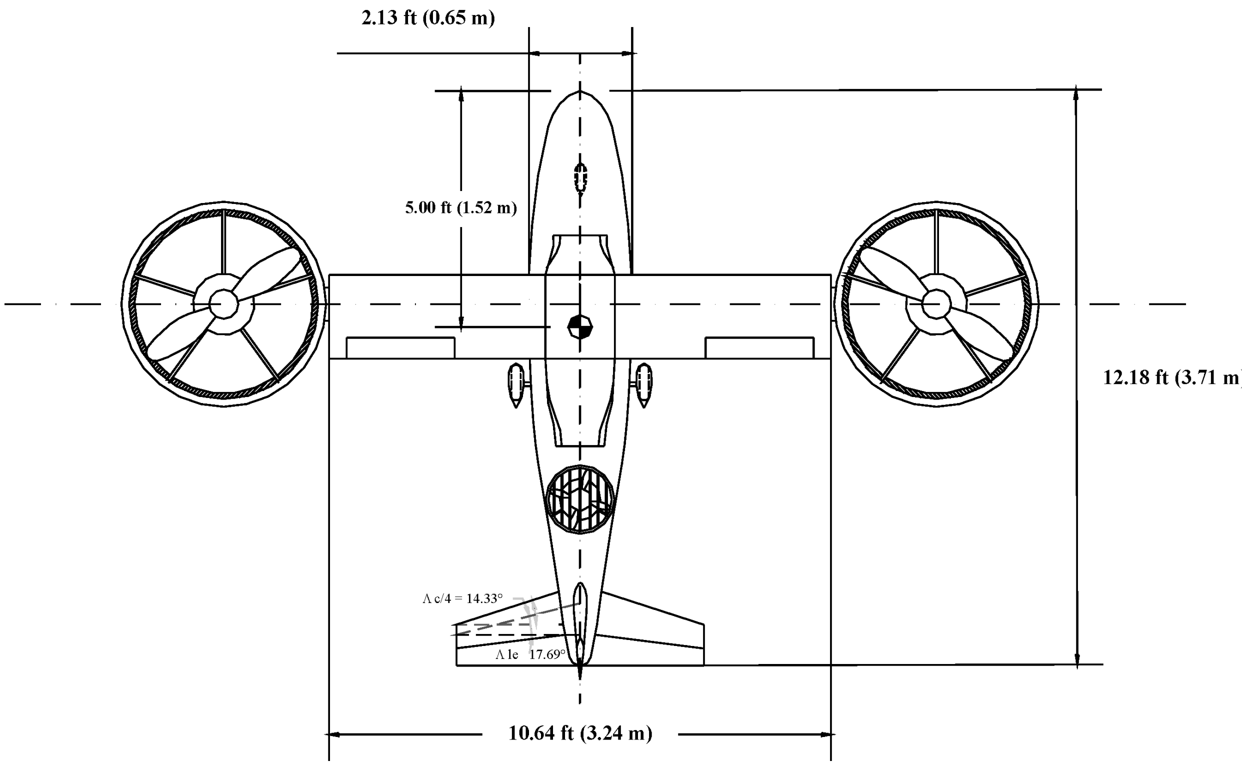

Fig. 5 Top view of the aircraft in hover mode.

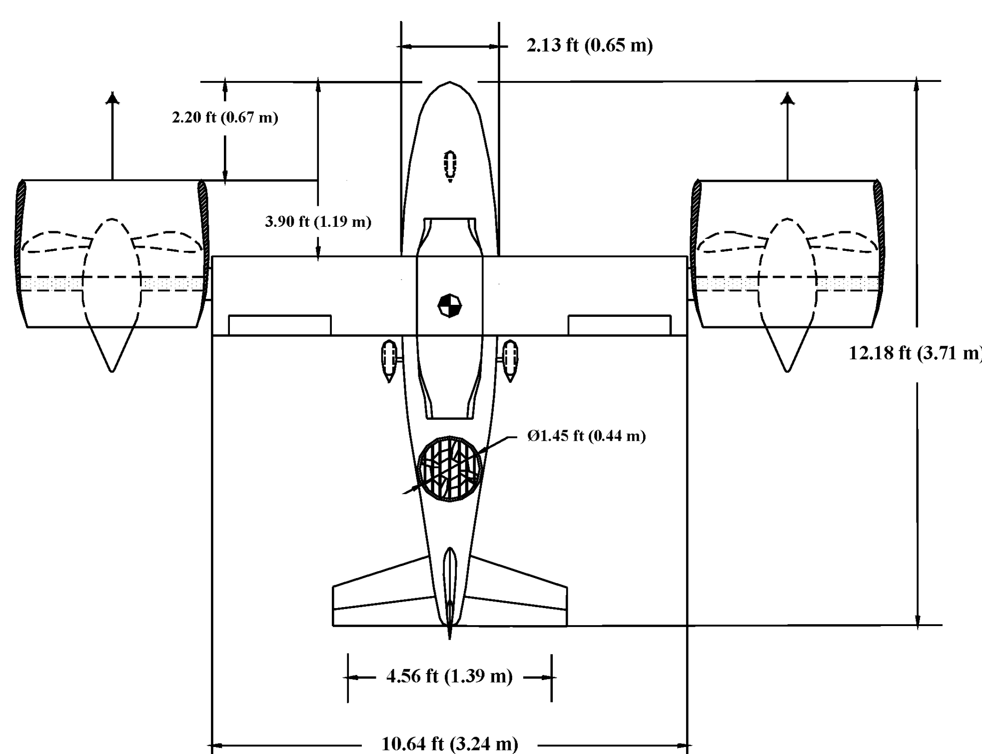

Fig. 6 Top view of the aircraft in forward flight mode.

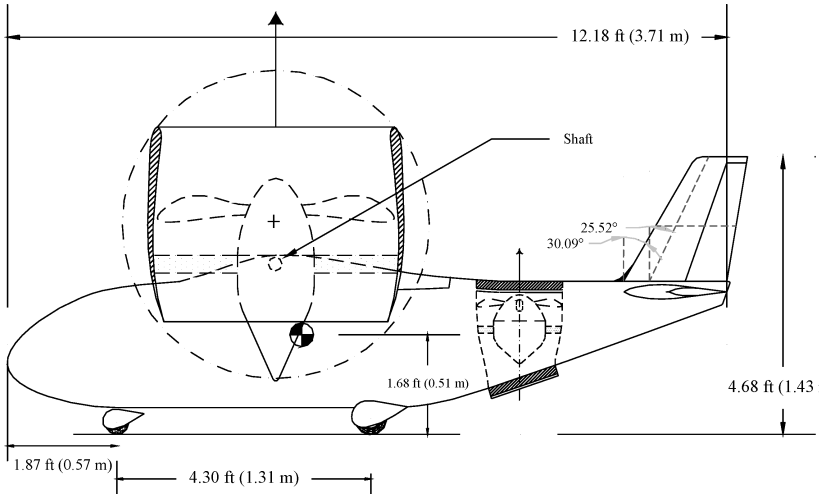

Fig. 7 Side view of the aircraft in hover mode.

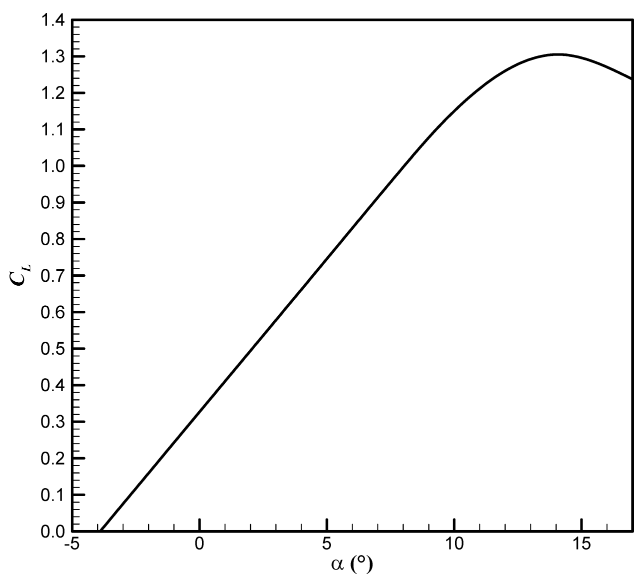

Fig. 8 Lift curve.

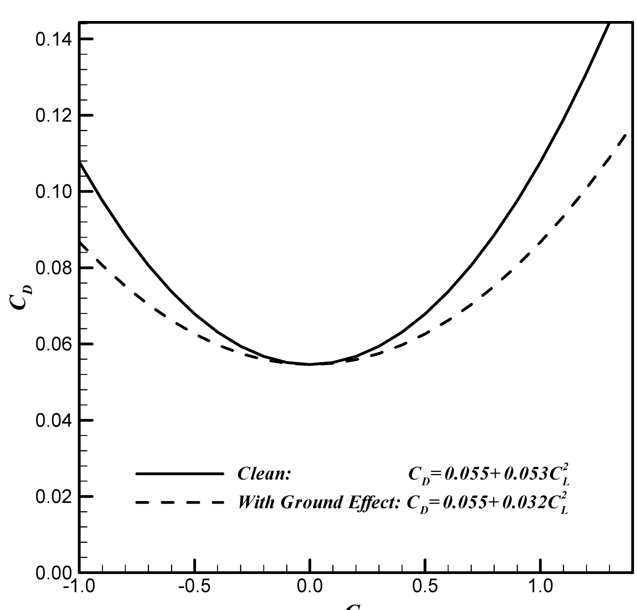

Fig. 9 Drag polar curves.

Table 7 Stability and control parameters

Parameter	Value
$\bar{X}_{\mathrm{c.g.}}$	0.62
$\bar{X}_{\mathrm{n.p.}}$	0.83
SM	0.21
$C_{L\alpha}$	4.591 rad^{-1}
$C_{D\alpha}$	0.6016 rad^{-1}
$C_{m\alpha}$	-0.9545 rad^{-1}
$C_{l\beta}$	-0.411 rad^{-1}
$C_{n\beta}$	0.722 rad^{-1}
$C_{y\beta}$	-0.6305 rad^{-1}

Configuration Layout

The fuselage is aerodynamically shaped, and it is 12.18 ft (3.72 m) long and 2.13 ft (0.65 m) in diameter. The bottom surface aft up-sweep angle is 19.76 deg. The distance between the aerodynamic centers of the wing and the tail surfaces is about 54% of the fuselage length. In Figs. 5 and 6 the top views of the aircraft in forward flight and hover modes are presented, and in Fig. 7 the side view of the aircraft in hover mode is shown. The calculated wetted surface areas and volumes are given in Table. 6. It is clear that the ducts make an important contribution to the total wetted surface area, thus, to the zero-lift drag of the aircraft.

Aerodynamics

The lift curve slope of the aircraft is estimated as $C_{L_\alpha} = 4.5107$ rad^{-1}, and the maximum lift coefficient is estimated as $C_{L,\max} = 1.3$. The zero-lift drag is calculated as $C_{D0} = 0.055$. The estimated lift curve of the aircraft is shown in Fig. 8. The estimated drag polars for the clean aircraft and for the aircraft on the ground are shown in Fig. 9.

Weights

The total weight of the aircraft is estimated as 227 lb (1009.7 N), and the c.g. location is estimated at 5.00 ft (1.52 m) behind the nose, which corresponds to the 62% $\bar{c}$ location. The component weights are as follows: wing, 12.92 lb (57.47 N); horizontal tail, 2.07 lb (9.21 N); vertical tail, 1.15 lb (5.12 N); fuselage, 29.54 lb (131.4 N); main landing gear, 19.5 lb (86.7 N); nose landing gear, 4.71 lb (20.95 N); main engines, 68.44 lb (304.42 N); aft engine, 19.16 lb (85.22 N); and camera, 17.64 lb (78.46 N).

Stability and Control

The neutral point is estimated at 5.37-ft (1.64 m) behind the nose, which corresponds to 83% $\bar{c}$ location. Then the static margin is calculated as $0.83 - 0.62 = 0.21$. The main stability and control

Table 8 Performance parameters

Parameter	Value
$V_{b.r.}$ at 6562 ft (2000 m)	61.58 kn (104 ft/s)
V_{max} at 6562 ft (2000 m, $P_{av} = 36$ hp)	146 kn (247 ft/s)
V_{stall} at 3281 ft (1000 m)	50 kn (84.45 ft/s)
Climb angle γ (sea level, $V = 66$ kn, $P_{av} = 39$ hp)	35 deg
Rate of climb (sea level, $V = 66$ kn, $P_{av} = 39$ hp)	3895 ft/min (1187 m/min)
Conventional takeoff ground roll (sea level, $P_{av} = 45$ hp)	167 ft (51m)
Conventional takeoff field length (sea level, $P_{av} = 45$ hp)	363 ft (111 m)
Conventional landing ground roll (sea level)	591 ft (180 m)
Conventional landing field length (sea level)	1262 ft (385 m)

parameters are listed in Table 7. The other stability derivatives, which are not shown in Table 7, are available in Ref. 29.

Performance

Some of the estimated performance parameters of the tilt-duct VTOL UAV are listed in Table 8.

Flight Control System Design

Initial flight mechanics analyses showed that this aircraft is inherently unstable during the hover and transition flights, which necessitate the implementation of a full authority automatic flight control system.[33]

Conclusions

A tilt-duct VTOL UAV concept is presented. The present design incorporates two ducted propellers attached to the wing tips. There is another propeller located inside the aft fuselage for pitch and yaw control during hover and transition. Currently, the tilt rotor concept is preferred for propeller-driven tilt-thrust vehicle designs. The tilt-rotor concept utilizes helicopter-type rotors, which utilize cyclic flapping, pitching, and lagging mechanisms. For a tilt-thrust aircraft designed for cruise, these types of features may be needed only during the transitional flight, which is a very short interval of the flight path. Therefore, their avoidance may be considered for future designs. Aerodynamically, tilt-rotor aircraft have a complicated flowfield, which may be responsible for some accidents. The tilt-duct concept separates the flowfields of the propellers and the wing. Therefore, it is aerodynamically simpler. The third engine at the rear may seem like adding to the cost and weight, but it may also be providing more reliable means for pitch and yaw control. Ducts increase the wetted surface area and weight of the aircraft, thus, they cause a drag increase. This may be compensated with the thrust increase because of the ducts and the ducts contribution to the lift by serving as ring wings.

It can be foreseen that in the future tilt-thrust vehicles may replace classical airplanes and helicopters. It can also be foreseen that in the future UAVs will have more applications than today, ranging from cargo planes to agricultural aircraft. For the development of safer, more reliable, and more economical tilt-thrust vehicles, more research is needed. A small VTOL UAV may serve as a low-cost research vehicle. Optimized design of ducted propellers can be considered among the future research topics.

Acknowledgments

The tilt-duct vertical takeoff and landing uninhabited aerial vehicle project was initiated at Middle East Technical University as a collaborative research effort. The authors would like to acknowledge the valuable contributions of two group members, Ersin Tulunay and Aycan Okan.

References

[1]McCormick, B. W., *Aerodynamics, Aeronautics and Flight Mechanics*, 2nd ed., Wiley, New York, 1995, Chap. 8, pp. 432–442.

[2]McCormick, B. W., *Aerodynamics of V/STOL Flight*, Dover, New York, 1999.

[3]Kohlman, D. L., *Introduction to V/STOL Airplanes*, Iowa State Univ. Press, Ames, IA, 1981.

[4]Hellman, H., *Helicopters and Other VTOLs*, 1st ed., Doubleday, Garden City, NY, 1970.

[5]Morris, W. B., McCormick, R. L., and Sinacori, J. B., "Moving-Base Simulator Study of an All-Mechanical Control System for VTOL Aircraft," *Journal of Aircraft*, Vol. 1, No. 1, 1964, pp. 41–45.

[6]Campbell, J. P., "Status of V/STOL Research and Development in the United States," *Journal of Aircraft*, Vol. 1, No. 3, 1964, pp. 97–106.

[7]Stepniewski, W. Z., and Schneider, J. J., "Design Philosophy and Operational Requirements of Subsonic VTOL Aircraft," *Journal of Aircraft*, Vol. 1, No. 3, 1964, pp. 148–156.

[8]Kriebel, A. R., "Theoretical Stability Derivatives for a Ducted Propeller," *Journal of Aircraft*, Vol. 1, No. 4, 1964, pp. 203–210.

[9]Dansby, T., Garrard, W. C. J., Ryle, D. M., and Sullivan, L. J., "V/STOL Development of the C-130 Hercules," *Journal of Aircraft*, Vol. 1, No. 5, 1964, pp. 242–251.

[10]Tanner, W. H., and Bergquist, R. B., "Some Problems of Design and Operation of a 250-Knot Compound Helicopter Rotor," *Journal of Aircraft*, Vol. 1, No. 5, 1964, pp. 252–259.

[11]Parlett, L. P., and Kirby, R. H., "Test Techniques Used by NASA for Investigating Dynamic Stability Characteristics of V/STOL Models," *Journal of Aircraft*, Vol. 1, No. 5, 1964, pp. 260–266.

[12]Stutz, R. G., and Price, G., "Agility Performance of Several V/STOL and STOL Aircaft," *Journal of Aircraft*, Vol. 1, No. 5, 1964, pp. 267–272.

[13]Hafner, R., "Domain of the Convertible Rotor," *Journal of Aircraft*, Vol. 1, No. 6, 1964, pp. 350–359.

[14]Seckel, E., *Stability and Control of Airplanes and Helicopters*, Academic Press, New York, 1964.

[15]Lindenbaum, B., and Fraga, D. E., "A Review of the US Tri-Service V/STOL Programs," *Military Applications of V/STOL Aircraft*, CP-126, AGARD, Oct. 1972.

[16]Dickmann, H. E., "Fundamentals of Annular Airfoil Theory (Nozzles in a Free Stream)," *Ingenieur Archiv*, II, 1940; translated by A. B. Finkelstein, L. Meyerhoff, and B. Zacharkiw, as PIBAL Rept. 353, Dept. of Aeronautical Engineering and Applied Mechanics, Polytechnic Inst. of Brooklyn, Armed Services Technical Information Agency, ASTIA AD 125091, Aug. 1956.

[17]Sacks, A. H., and Burnell, J. A., "Ducted Propellers—A Critical Review of the State of the Art," *Progress in Aeronautical Sciences*, edited by A. Ferri, D. Küchemann, and L. H. G. Sterne, Vol. 3, Pergamon Press, New York, 1962, pp. 85–135.

[18]Morgan, W. B., "A Theory of the Ducted Propeller with a Finite Number of Blades," Inst. of Engineering Research, Ser. 82, Contract 222(30), Univ. of California, Berkeley, CA, May 1961; also 4th Naval Symposium on Naval Hydrodynamics: Propulsion, Hydroelasticity, Aug. 1962, Washington, DC, Office of Naval Research and the Webb Inst. of Naval Architecture, edited by B. L. Silverstein, Dept. of the Navy, Supt. of Docs., U.S. Govt. Print. off., 1964.

[19]Ordway, D. E., Sluyter, M. M., and Sonnerup, B. O. U., "Three-Dimensional Theory of Ducted Propellers," TAR-TR-602, Therm Advanced Research, Ithaca 1, New York, Aug. 1960.

[20]Küchemann, D., and Weber, J., *Aerodynamics of Propulsion*, McGraw–Hill, New York, 1953; Chap. 6, pp. 125–140.

[21]Weissinger, J., "Remarks on Ring Airfoil Theory," Inst. für Angewandte Mathematik der Technischen Hochschule Karlsruhe, European Office Air Research and Development Command, Contract AF 61(514)-1207, Air Force Office of Scientific Research, AFOSR TN 58-224, Armed Services Technical Information Agency, ASTIA AD 154127, Jan. 1958.

[22]Kriebel, A. R., and Mendenhall, M. R., "Predicted and Measured Performance of Two Full-Scale Ducted Propellers," CAL/USAAVLABS Symposium Proceedings on Aerodynamic Problems Associated with V/STOL Aircraft, Cornell Aeronautical Lab., Inc., Ithaca, New York, U.S. Army Aviation Material Lab., Fort Eustis, VA, June 1966.

[23]Thompson, J. F., and Roberts, S. C., "Shrouded Propeller Research at Mississippi State University Leading to Application on the United States Army XV-11A," CAL/USAAVLABS Symposium Proceedings on Aerodynamic Problems Associated with V/STOL Aircraft, Cornell Aeronautical Lab., Inc., Ithaca, New York, U.S. Army Aviation Material Lab., Fort Eustis, VA, June 1966.

[24]Newmann, S., *The Foundations of Helicopter Flight*, Edward Arnold, London, United Kingdom, 1994, Chaps. 3, 4.

[25]Raymer, D. P., *Aircraft Design: A Conceptual Approach*, 2nd Ed., AIAA Education Series, AIAA, Washington, DC, 1992.

[26]Roskam, J., *Airplane Design*, 2nd printing, Roskam Aviation and Engineering Corp., Pts. 1–8, Ottawa, KS, 1990.

[27]Torenbeek, E., *Synthesis of Subsonic Airplane Design*, Delft Univ. Press, Delft, The Netherlands, 1976.

[28]Advanced Airplane Analysis (AAA) Program, Ver. 2.2, DAR Corp., Lawrence, Kansas, 1999.

[29]Armutcuoğlu, Ö., "The Conceptual Design of a Tilt-Duct VTOL UAV," M.S. Thesis, Dept. of Aeronautical Engineering, Middle East Technical Univ., Ankara, Turkey, Dec. 2000.

[30]Eppler, Richard, *Airfoil Design and Data*, Springer–Verlag, Heidelberg, Germany, 1990.

[31]*Jane's All The World's Aircraft*, Jane's Information Group, Surrey, United Kingdom, 1998.

[32]Lan, C. E., and Roskam, J., *Airplane Aerodynamics and Performance*, Roskam Aviation and Engineering Corp., Ottawa, Kansas, 1980.

[33]Okan, A., Tekinalp, O., and Kavsaoğlu, M. S., "Flight Control of a Tilt-Duct VTOL UAV," AIAA Paper 2002-3466, May 2002.